Study on the persistent luminescence of diopside nanotracers CaMgSi2O6: Eu2+ , Mn2+, Pr3+

Céline Rosticher, Corinne Chaneac, Adrie Bos, Bruno Viana

Study on the persistent luminescence of diopside nanotracers $CaMgSi_2O_6$: Eu^{2+}, Mn^{2+}, Pr^{3+}

Céline Rosticher [1], Corinne Chanéac[1*], Adrie Bos[2], Bruno Viana[3*]

[1] *Sorbonne Universités, UPMC Univ. Paris 06, CNRS, Collège de France, Laboratoire de Chimie de la Matière Condensée de Paris, 11 place Marcelin Berthelot, 75005 Paris, France*

[2] *Delft University of Technology Faculty of Applied Sciences, department Radiation Science & Technology Mekelweg 15, 2629JB Delft , The Netherlands*

[3] *PSL Research University, Chimie ParisTech − CNRS, Institut de Recherche de Chimie Paris, 75005 Paris, France, 11 rue Pierre et Marie Curie, 75231 Paris Cedex 05, France*

ABSTRACT

We present a study on diopside nanotracers with persistent luminescence properties in the red-near IR range for small animal imaging. In this paper we have focused our attention on improving the persistent luminescence of diopside nanoparticles doped with transition metal and lanthanide ions. Earlier study showed that Pr^{3+} is the most suitable Ln^{3+} electron trap in Eu^{2+}, Mn^{2+} doped diopside lattice. Here, we report an optimization of both chemical composition of $CaMgSi_2O_6$ matrix and Eu, Mn, Pr doping elements to improve persistent luminescence. These new inorganic persistent luminescent nanoparticles (i-PLNPs) emit in the red-near infrared range for several hours and can master the difficulties due to the biological environment.

Keywords: diopside, persistent luminescence, *in vivo* imaging, near infrared emission, nanotracers

1. INTRODUCTION

Persistent luminescence materials are used in many applications ranging from traffic signs, emergency signage, watches, clocks, textile printing, security inks to photovoltaic applications and some of them represents the commercial development of these persistent phosphors. In last few years, more than two hundreds combinations of host materials and activator ions have been depicted, of which around 20% are devoted to divalent europium (Eu^{2+}) and codopant ions [1].

Bioimaging is a rapidly expanding field where progress is constant and has been successfully demonstrated. Persistent luminescence, particularly covering red and NIR light emitting materials, has new application fields in bioimaging for *in vivo* and *in vitro* studies [2-8]. The first requirement is to obtain nanomaterials in a regular shape with size which should not exceed 100 nm. Main recent focus is on red-near infrared persistent luminescence nanoparticles doped with transition metal (Mn^{2+} and Cr^{3+})[9,10] and few are in lanthanides doped sensors (such as Eu^{3+} , Pr^{3+} , Sm^{3+}, Nd^{3+}) [11,13]. For *in vivo* purposes, such sensors should overcome two main difficulties caused by the biological environment: adsorption and autofluorescence from irradiated tissues [14,15].

In 2007 Le Masne de Chermont *et al.* reported the synthesis of inorganic luminescent silicates nanoparticles $Ca_{0.2}Zn_{0.9}Mg_{0.9}Si_2O_6$: Eu^{2+}, Mn^{2+}, Dy^{3+} [16]. They showed some good persistent luminescence properties in the red-near infrared range at 680 nm, therefore avoiding the tissues' absorption and autofluorescence as they were injected after UV excitation and still exhibited luminescence for several minutes [16]. Following that zinc free silicates $Ca_xMg_ySi_2O_6$ doped with Eu^{2+}, Mn^{2+}, Dy^{3+} was developed using a sol gel method similar to the Stöber process [17,18]. A very strong persistent luminescence at 680 nm, suitable for *in vivo* imaging, has been obtained for $Ca_{0.3}Mg_{1.7}Si_3O_8$: Eu^{2+} (1%), Mn^{2+} (5%), Dy^{3+} (2%) 50 nm sized nanoparticle.

To further improve the optical properties of $CaMgSiO_2$ sensors, the role of Ln^{3+} codoping ions has been investigated[2]. Codoping with Ln^{3+} ions showed two main impacts on the optical properties of the doped materials: (i) The localization of the doping trivalent ions preferably in Ca^{2+} or Mg^{2+} sites (the two available cationic sites in silicate structure)

depending on its ionic radius influences the localization of Mn^{2+} ions responsible of the persistent luminescence at 580 and 680 nm, corresponding to Mn^{2+} in Ca^{2+} and Mg^{2+} sites respectively [17,19,20]. When the trivalent rare earth presents a ionic radius similar to the one of calcium (1 Å), like Pr^{3+} ions (1.01 Å), Mn^{2+} occupies preferably calcium sites. This favored occupation of Ca^{2+} sites by Pr^{3+} ions leads to a major occupation of magnesium sites by Mn^{2+} ions (labelled Mn_{Mg}). It has been proved that $Mn^{2+}{}_{Mg}$ was the luminescent center [17,19], then the increasing of $Mn^{2+}{}_{Mg}$/ $Mn^{2+}{}_{Ca}$ ratio renders $Mn^{2+}{}_{Mg}$ emission at 680 nm more intense. (ii) It was also previously reported that Ln^{3+} ions act as electron traps and that Pr^{3+} provided a more intense luminescence than Dy^{3+} in the case of $CaMgSiO_2$: Eu^{2+}, Ln^{3+} excited under UV and X-rays [2, 17]. Maldiney *et al.* showed that the wavelength-resolved thermoluminescence (TSL) spectrum of Pr^{3+} presented an intense peak at 353K. The peak position, just above the ambient temperature, and its strong intensity can explain why a longer and more intense luminescence was observed for codoping with Pr^{3+} [2]. Different trap depths were measured for oxygen vacancies and Ln^{3+} ions: $E(V_o) = 0.95$ eV, $E(Ce^{3+}) = 0.4$ eV, $E(Pr^{3+}) = 0.7$ eV, $E(Nd^{3+}) = 0.92$ eV et $E(Dy^{3+}) = 1.7$ eV [2]. Dy^{3+} traps appear to be much deeper than Pr^{3+} traps. Then detrapping of an electron localized on Pr^{3+}-trap would be thermally favored. A 0.7 eV trap depth appears as a good choice to obtain stronger and longer persistent luminescence at room temperature.

We present hereafter a study on $Ca_xMg_ySi_2O_6$ silicates nanoparticles doped with Eu^{2+}, Mn^{2+}, Pr^{3+} to further improve luminescence properties. We focus our attention on new preparation method compared to previous work that led to too large and aggregated nanoparticles. Structural and optical properties of nanomaterials have been performed for various Ca/Mg/Si molar ratio and doping ratio.

2. EXPERIMENTAL

2.1 Sample synthesis

Maldiney *et al.* reported the synthesis of diopside nanoprobes by sol gel process using a acid catalysis [2,16,21]. Nanoparticles are directly growing inside a silica matrix which plays the role of silica source and limits the crystal growth during high temperature treatment. However as-obtained nanoparticles tend to exhibit a high diameter and to form aggregates which is unfavorable from the point of view of *in vivo* imaging applications. In the present work, diopside nanoparticles were synthetized according to the procedure reported in Ref. [17] using a sol gel method inspired from the Stöber process. This method enables to obtain non-aggregated silica-diopside core-shell type nanoparticles with smaller size.

In a typical synthesis, two different solutions are prepared: the first one S_1 is obtained by mixing absolute ethanol (92 mL), water (14 mL) and NH_4OH solution (30%, 6 mL), and the second one S_2 by dissolving matrix precursors $Mg(NO_3)_2.6H_2O$, $CaCl_2$, and tetraethyl orthosilicate (TEOS) with doping precursors $MnCl_2$, $EuCl_3.6H_2O$, $PrCl_3$ in absolute ethanol (8mL). Then S_2 is added to S_1 drop by drop while stirring at room temperature. The obtained sol is stirred vigorously for 24h, then dried at 90°C for 30h, and annealed at 1150°C for 10h under reductive atmosphere (95% N_2, 5% H_2). This last step is essential to reduce Eu^{3+} in Eu^{2+} and to allow the persistent luminescence properties. The as-obtained nanoparticles are coated by an amorphous silica layer and are aggregated. The samples were treated with NH_5F_2 0.5M for 1h to reduce the thickness of the amorphous silica coating [17]. The product is then thoroughly washed with water and dried under air. Table 1 resumes the samples used in this study with their chemical compositions, crystalline structures and optical properties.

2.2 Structural and optical characterizations

Powder X-ray diffraction (PXRD) study was performed on a Bruker D8 Advance diffractometer using Cu-Kα radiation (λ = 1.5418 Å) at 45 kV and 40 mA, 0.0046°θ step size and 0.5s step time over a range of 10°θ to 80°θ. Transmission electron microscopy (TEM) images were acquired with a FEI Tecnai 120 Twin microscope operating at 120 kV and equipped with a high resolution Gatan Orius CCD 4 k 64 k numeric camera. Excitation and emission spectra were measured with a Varian Cary Eclipse Fluorescence spectrophotometer at room temperature. Persistent luminescence spectra were recorded after 2 minutes irradiation with UV light, and the resulting signal was collected via an optical fiber by Roper Scientific Pixis 100 CCD camera cooled at -68°C coupled with an Acton SpectraPro 2150i spectrometer for spectral analysis. Thermoluminescence (TL) measurements were performed with a Risø TL/OSL reader model TL/OSL-DA-15A/B with an EMI 9635QA PM tube. TL glow curves were standard measured at heating rate of 5°C/s. TL emission spectra were measured using an UV-VIS spectrometer (Avantes, PC2000). For the emission spectra measurements the samples were irradiated with 340 nm UV light for 2 minutes.

Table 1. Chemical compositions, crystalline structures and optical properties of obtained samples.

Composition	Crystalline structure	Persistent luminescence intensity*	Abbreviation
$Ca_{0.3}Mg_{1.7}Si_3O_8$: Eu^{2+} (1%), Mn^{2+} (5%), **Dy^{3+}** (2%)	clinoenstatite	m.s.	A
$Ca_xMg_ySi_2O_6$: Eu^{2+} (0.5%), Mn^{2+} (2.5%), **Pr^{3+}** (1%) Serie			C_xM_y
$CaMgSi_2O_6$: Eu^{2+} (0.5%), Mn^{2+} (2.5%), Pr^{3+} (1%)	diopside	m.s.	C_1M_1
$Ca_{0.8}Mg_{1.2}Si_2O_6$: Eu^{2+} (0.5%), Mn^{2+} (2.5%), Pr^{3+} (1%)	diopside	m.s.	$C_{0.8}M_{1.2}$
$Ca_{0.6}Mg_{1.4}Si_2O_6$: Eu^{2+} (0.5%), Mn^{2+} (2.5%), Pr^{3+} (1%)	diopside-clinoenstatite	s.	$C_{0.6}M_{1.4}$
$Ca_{0.4}Mg_{1.6}Si_2O_6$: Eu^{2+} (0.5%), Mn^{2+} (2.5%), Pr^{3+} (1%)	clinoenstatite	w.	$C_{0.4}M_{1.6}$
$Ca_{0.2}Mg_{1.8}Si_2O_6$: Eu^{2+} (0.5%), Mn^{2+} (2.5%), Pr^{3+} (1%)	clinoenstatite	v.w.	$C_{0.2}M_{1.8}$
$Mg_2Si_2O_6$: Eu^{2+} (0.5%), Mn^{2+} (2.5%), Pr^{3+} (1%)	clinoenstatite	v.w.	M_2
$CaMgSi_2O_6$: Eu^{2+} (1%), Mn^{2+} (5%), Pr^{3+} (2%)	diopside	v.s.	C_1M_1-2

**v.w.: very weak, w.: weak, m.s.: medium strong, s.: strong, v.s.: very strong.*

3. RESULTS AND DISCUSSION

3.1 Shape and morphology

The nanoparticles obtained are spherical and present an average diameter of 50 nm. After treatment with NH_5F_2 0.5M for one hour, the amorphous silica layer surrounding the nanoparticles was efficiency reduced to a thickness of 2.7nm [17].

3.2 Optical Emission

Doped with Eu^{2+}, Mn^{2+} and Pr^{3+} to insure efficient pumping in the UV and efficient emission in the red/near IR range, the emission spectrum of $CaMgSi_2O_6$: Eu^{2+} (1%), Mn^{2+} (5%), Pr^{3+} (2%) exhibits three emission peaks at 597, 614 and 630 nm corresponding to $^3P_0 \rightarrow {}^1D_2$ and $^3P_0 \rightarrow {}^3H_6$ transition of Pr^{3+} ion, and one large emission band at 680nm corresponding to Mn^{2+} emission (figure 1). The excitation spectrum shows two domains: one band at about 250 nm corresponding to $O^{2-} \rightarrow Mn^{2+}_{Ca}$ charge transfer, a large band between 275 and 450 nm attributed to *4f-5d* transition of Eu^{2+} and additional bands/peaks corresponding to the 3*d-3d* transitions of Mn^{2+} ions.

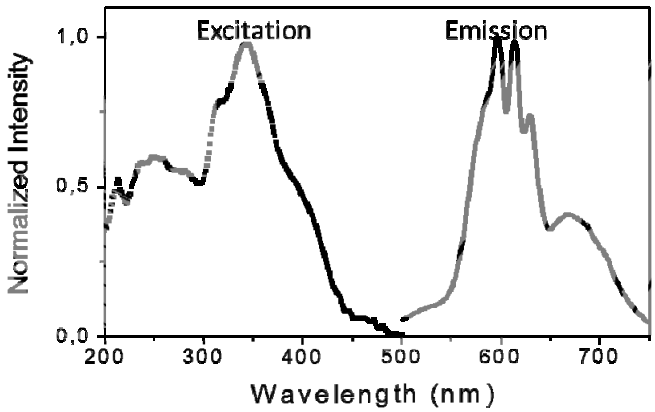

Figure 1. Excitation and emission spectra of C_1M_1 (Pr2%) compound (see table 1) – λ_{exc} = 350 nm, λ_{em} = 614 nm.

3.4 Red-NIR persistent luminescence

In the aim of improving the persistent luminescence and studying the chemical composition influence on the persistent luminescence properties of $CaMgSi_2O_6$: Eu^{2+}, Mn^{2+}, Pr^{3+}, we modified Ca/Mg/Si molar ratio by varying the $(C_2H_5O)_4Si$ (TEOS) initial quantity. Only Ca/Mg/Si molar ratio modifications brought valuable informations and are presented below.

$Ca_xMg_ySi_2O_6$ silicates belong to the pyroxenes group whom general formula is $M2M1(SiO_3)_2$, with M1 a small cation surrounded by 6 oxygen atoms and M2 a larger cation surrounded by 8 oxygen atoms. Small ions, like Mg^{2+}, Fe^{2+} or Zn^{2+} always occupy M1 sites [22,23]. When they are the only cations in the matrix, they can occupy M2 site too and form an orthopyroxene phase (enstatite $Mg_2Si_2O_6$), with orthorhombic symmetry. If some larger cation is present in the matrix, like Ca^{2+} or Na^{+}, then it necessarily occupies M2 cationic site. The symmetry becomes then monoclinic by lateral sliding of elementary chains. Those compounds form the clinopyroxenes groups and the main ones are the diopside $CaMgSi_2O_6$.

Therefore changing Ca/Mg/Si molar ratio in $Ca_xMg_ySi_2O_6$ silicates is equivalent to modifying the crystalline structure of the samples. XRD diagrams of $Ca_xMg_ySi_2O_6$ silicates doped with Eu^{2+}, Mn^{2+} and Pr^{3+} show an evolution from clinoenstatite phase $Mg_2Si_2O_6$ to a diopside phase $CaMgSi_2O_6$ with Ca/Mg molar increasing ratio (figure 2).

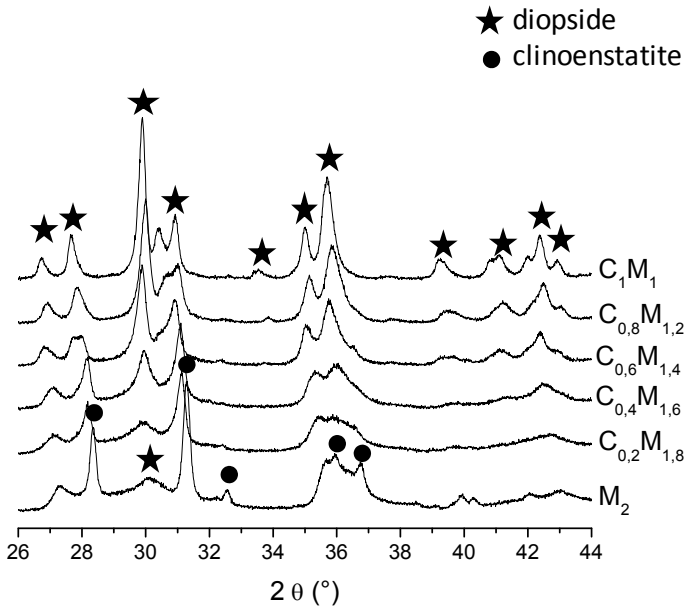

Figure 2. PXRD patterns of $Ca_xMg_ySi_2O_6$: Eu^{2+}, Mn^{2+} and Pr^{3+} silicates. See table 1 for the respective compositions.

The persistent luminescence spectra of all $Ca_xMg_ySi_2O_6$: Eu^{2+} (0.5%), Mn^{2+} (2.5%), Pr^{3+} (1%) compounds recorded after switching off the UV excitation exhibit the same three characteristic emission bands at 480, 580 and 680 nm (not shown here). The band at 480 nm has been attributed to the allowed $4f^65d^1 \rightarrow 4f^7$ transition of Eu^{2+}, whereas the bands at 580 and 680 nm correspond to the $^4T_1 \rightarrow {}^6A_1$ transition of Mn^{2+} in Ca^{2+} and Mg^{2+} sites respectively [13,14]. Following the previously reported $Ca_xMg_ySi_2O_6$ compound doped with Eu^{2+}, Mn^{2+} and trivalent dysprosium, no characteristic Pr^{3+} emission was observed [17]. However, there are few differences in the luminescent behavior of $Ca_xMg_ySi_2O_6$ doped with Eu^{2+}, Mn^{2+}, Pr^{3+} or Eu^{2+}, Mn^{2+}, Dy^{3+} excepted that the persistent luminescence is much more intense for Pr^{3+} doped silicates. This confirms that Pr^{3+} ions have an effect on the persistent luminescence mechanism. Notice also an important increase of intensity for Eu^{2+} emission band at 480 nm.

With Ca/Mg molar ratio variation, persistent luminescence intensity in NIR range increases and the ratio of intensities of the band at 580 nm to the band at 680 nm also increases. Variation in Ca/Mg molar ratio has then an influence on Mn^{2+} distribution in the two cationic sites and on the persistent luminescence intensity. Pr^{3+} ions present ionic radius of 1.01 Å, larger than Mg^{2+} (0.72) or Ca^{2+} ions (1 Å) [24]. In $Ca_xMg_ySi_2O_6$ silicates, Pr^{3+} ions are only hosted in Ca^{2+} sites. This leads to a preferred occupation of Mg^{2+} sites by Mn^{2+} ions. High Ca/Mg molar ratio facilitates the insertion of Pr^{3+} ions in the silicate structure and favors the Mn^{2+}_{Mg} luminescent centers. Therefore, the luminescence becomes most intense and persistent when the Ca/Mg molar ratio is the highest for $Ca_xMg_ySi_2O_6$: Eu^{2+}, Mn^{2+}, Pr^{3+}

compounds. Indeed the most intense and persistent sample was obtained in $Ca_{0,6}Mg_{1,4}Si_2O_6$: Eu^{2+} (0.5%), Mn^{2+} (2.5%), Pr^{3+} (1%).

At this stage it is important to notice that the optimization of the persistent luminescence leads to only a small intensity difference in comparison to the composition $CaMgSi_2O_6$: Eu^{2+} (0.5%), Mn^{2+} (2.5%), Pr^{3+} (1%) reported in Ref [2]. $Ca_{0,6}Mg_{1,4}Si_2O_6$: Eu^{2+} (0.5%), Mn^{2+} (2.5%), Pr^{3+} (1%) sample presents a mixed clinoenstatite/diopside crystalline structure, and the reproducibility of the composition is quite difficult. Hence, this optimization by changing Ca/Mg molar ratio is not significant and not enough beneficial to be retained.

A second method to enhance the persistent luminescence of Eu^{2+}, Mn^{2+}, Pr^{3+} doped silicates is to vary the doping ratio of each dopant. Best results were obtained for $CaMgSi_2O_6$: Eu^{2+} (1%), Mn^{2+} (5%), Pr^{3+} (2%) sample (C_1M_1-2) where Eu^{2+}, Mn^{2+}, Pr^{3+} doping ratios have been increased twice. The persistent luminescence properties of this sample was then compared to the most intense sample $Ca_{0,6}Mg_{1,4}Si_2O_6$: Eu^{2+} (0.5%), Mn^{2+} (2.5%), Pr^{3+} (1%) and to $CaMgSi_2O_6$: Eu^{2+} (0.5%), Mn^{2+} (2.5%), Pr^{3+} (1%) reported in Ref [2]. For Eu^{2+}, Mn^{2+}, Pr^{3+} doping, the strongest effect on the persistent luminescence was observed for the diopside structure with a high doping ratio: $CaMgSi_2O_6$ doped Eu^{2+} (1%), Mn^{2+} (5%), Pr^{3+} (2%) as seen in Figure 3.

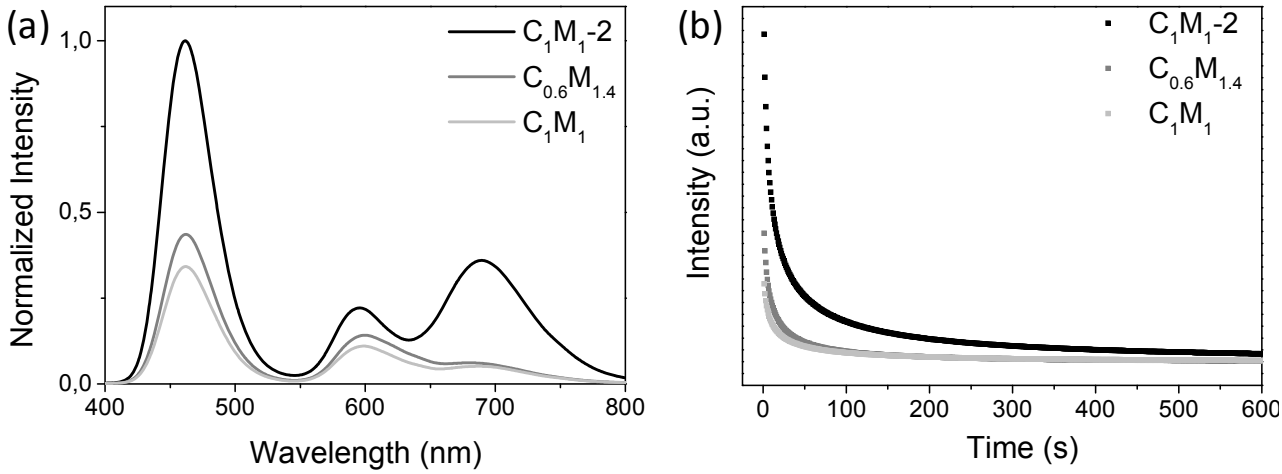

Figure 3. (a) Persistent luminescence spectra and (b) decays of the persistent luminescence of C_1M_1, $C_{0.6}M_{1.4}$ and C_1M_1-2 compounds – λ_{exc} = 365 nm – excitation time = 2 min (see table 1 for the samples composition).

3.4 Dy^{3+} *vs* Pr^{3+} as trivalent codopant for enhanced persistent luminescence in the hosts

In a previous study on Dy^{3+} codoped silicates, $Ca_{0.3}Mg_{1.7}Si_3O_8$: Eu^{2+} (1%), Mn^{2+} (5%), Dy^{3+} (2%), (referred here as sample A (Dy^{3+})) was determined to be an optimal composition [17]. We present hereafter a comparison of the clinoenstatite $Ca_{0.3}Mg_{1.7}Si_3O_8$: Eu^{2+} (1%), Mn^{2+} (5%), Dy^{3+} (2%) versus diopside $CaMgSi_2O_6$: Eu^{2+} (1%), Mn^{2+} (5%), Pr^{3+} (2%) compounds.

The persistent luminescence spectra of both samples exhibit the same three emission bands at 480, 580 and 680 nm corresponding to Eu^{2+}, Mn^{2+}_{Ca} and Mn^{2+}_{Mg} emissions respectively [17]. This means that the persistent luminescence mechanisms are similar for Pr^{3+} and Dy^{3+} doping, where Mn^{2+} ions remains the luminescent centers. Although identical in emission wavelength, persistent luminescence of $CaMgSi_2O_6$: Eu^{2+} (1%), Mn^{2+} (5%), Pr^{3+} (2%) is up to seven times more intense than $Ca_{0.3}Mg_{1.7}Si_3O_8$: Eu^{2+} (1%), Mn^{2+} (5%), Dy^{3+} (2%). This stays in agreement with the previous work on the energy level position of the Dy^{3+} versus Pr^{3+} cations ref. [2].

The wavelength-resolved TSL spectra of $Ca_{0.3}Mg_{1.7}Si_3O_8$: Eu^{2+} (1%), Mn^{2+} (5%), Dy^{3+} (2%) (sample A) and $CaMgSi_2O_6$: Eu^{2+} (1%), Mn^{2+} (5%), Pr^{3+} (2%) (sample C_1M_1-2) recorded after switching off the UV excitation are presented in figure 4. Peaks appear at the same temperature range (130°C) meaning that the similar electron traps are involved but the emission spectra are different. Lecointre et *al.* showed that Mn^{2+} and Eu^{2+} act as hole-traps in these compounds, whereas trivalent ions (*i.e.* Dy^{3+}, Pr^{3+}) act as electron-traps [19]. More important is the difference on the

bandgap values for the two hosts that can explain the observed behavior. The bandgap difference about 0.5eV [2, 20] is reported between clinoenstatite and diopside hosts.

On sample A (left on Figure 4 presenting the wavelength-resolved TSL spectra), peaks are mostly located at 680nm, which means that they originate almost exclusively from Mn^{2+} ions in Mg^{2+} site. This indicates that Mn^{2+} ion in Mg^{2+} site is a much better hole trap ($Mn^{2+} + h^{+} \rightarrow Mn^{3+}$) than Mn^{2+} ion in Ca^{2+} site. The same observation can be made for sample C_1M_1-2 even if some small emission is observed at about 580 nm. This correlates with the persistent luminescence spectra where the emission band at 680 nm is predominant for Mn^{2+} emission as seen in Figure 3.

The thermoluminescence (TSL) starts at 70°C and a maximum is found at 130°C in both cases. The TSL peak is broad, observed from 70°C to 270°C. Yet, at 200°C, the signal could correspond to the participation of oxygen vacancies as electron traps. Keeping the same matrix as in Ref. [2], smaller trap depths obtained for Pr^{3+} ions (0.7 eV) are favorable in comparison to the deeper traps obtained for Dy^{3+} cations (1.7 eV). Here, between the two samples A and C_1M_1-2, the difference is not only the nature of rare earth cations (Dy^{3+}/Pr^{3+}) but also the crystallinity (clinoenstatite or diopside) of the matrix which presents different bandgap energy.

In addition for sample C_1M_1-2 ($CaMgSi_2O_6$: Eu^{2+} (1%), Mn^{2+} (5%), Pr^{3+} (2%)) wavelength-resolved TSL spectra presents a peak located at 480 nm with high intensity (see figure 4.B). Eu^{2+} also plays the role of hole trap ($Eu^{2+} + h^{+} \rightarrow Eu^{3+}$) and appears as the favored recombination center. After recombination energy transfer toward Mn^{2+} may occur. This behavior is in agreement with the persistent luminescence spectra where the emission band at 480 nm is very intense.

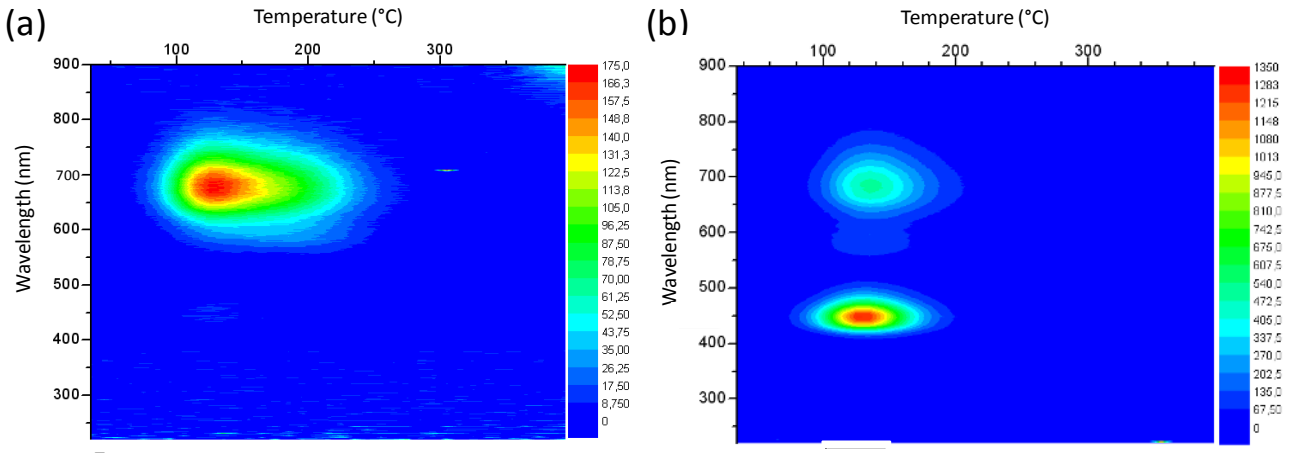

Figure 4. Wavelength-resolved TSL spectra of sample A and sample C_1M_1-2. See table 1 for the samples composition.

CONCLUSIONS

$CaMgSi_2O_6$ doped Eu^{2+}, Mn^{2+}, Pr^{3+} nanoparticles were prepared by a sol–gel method inspired by Stöber process in order to optimize red-near infrared persistent luminescence of nanoparticles reported in Refs [2, 17]. Materials with different Ca/Mg/Si molar ratios and different doping ratios have been prepared. Diopside structure $CaMgSi_2O_6$ shows enhanced persistent luminescence when doped with Eu^{2+} (1%), Mn^{2+} (5%), Pr^{3+} (2%). When compared to a previous study on Eu^{2+}, Mn^{2+}, Dy^{3+} doping [17], this composition proved to be more efficient for persistent luminescence purposes. Pr^{3+} ions provide electron trap levels about 0.7 eV below the conduction band edge, which allows optimal electron release and recombination at room temperature responsible for the highest persistent luminescence. The nanoparticles size (53 nm) associated to the easy surface modification can lead to a novel near-infrared optical nanoprobe usable for real-time optical imaging in small animals.

ACKNOWLEDGMENTS

We thank Patrick Le Griel for his help during TEM experiments. This work was supported by the French Research National Agency (ANR) in the frame of its program in Nanosciences and Nanotechnologies (Natlurim project n°ANR-08-NANO-025).

REFERENCES

[1] Van den Eeckhout, K., Poelman, D., Smet, P. "Persistent luminescence in non-Eu^{2+}-doped compounds: a review"; Materials 6, 7, 2789–2818 (2013).

[2] Maldiney, T., Lecointre, A., Viana, B., Bessière, A., Bessodes, M., Gourier, D., Richard, C., Scherman, D. "Controlling electron trap depth to enhance optical properties of persistent luminescence nanoparticles for in vivo Iimaging"; J. Am. Chem. Soc. 133, 11810–11815 (2011).

[3] Junpeng, S., Xia, S., Jinlei, L., Huizi, M., Jiangshan, S., Yanke, Y., Hongwu, Z. "Multifunctional NIR-emitting long-persistence luminescent nanoprobes for drug delivery and targeted tumor imaging"; Biomaterials, 37, 260–270 (2014).

[4] Xiaoyan, F., Chunlin, L., Junpeng, S., Huizi, M., Jia, X., Hongwu, Z. "Long persistent near infrared luminescence nanoprobes $LiGa_5O_8$:Cr-PEG-OCH_3 for in vivo imaging"; Optical Materials, 36, 1792–1797 (2014).

[5] Chuang, Y.J., Zipeng, Z., Fan, Z., Liu, F., Mishra, J.P., Tang, W., Chen, H., Huang, X., Wang, L., Chen, X., Xie, J. , Pan, Z. "Photostimulable near-infrared persistent luminescent nanoprobes for ultrasensitive and longitudinal deep-tissue bio-imaging"; Theranostics, 4, 11 (2014).

[6] Maldiney, T., Bessiere, A., Seguin, J., Teston, E., Sharma, S., Viana, B., Bos, A., Dorenbos, P., Bessodes, M., Gourier, D., Scherman, D., Richard, C. "The in vivo activation of persistent nanophosphors for optical imaging of vascularization, tumours and grafted cells"; Nature Mater., 13(4), 418–426 (2014).

[7] Jaque, D., Richard, C., Viana, B., et al. "Inorganic nanoparticles for optical bioimaging" doi: 10.1364/AOP.8.000001, Vol. 8, No. 1 / March 2016 /Advances in Optics and Photonic (2016).

[8] Viana, B., Sharma, S. K., Maldiney, T. et. al., "Long term in vivo imaging with Cr3+ doped spinel nanoparticles exhibiting persistent luminescence, J. Luminescence, 170, 3, 879-887 (2016).

[9] Bessiere, A.; Sharma, S. K.; Basavaraju, N.; Viana, B. et al."Storage of Visible Light for Long-Lasting Phosphorescence in Chromium-Doped Zinc Gallate" Chemistry of Materials: 26, 3 1365-1373, (2014).

[10] Xu, J.; Tanabe, S.; Sontakke, A., et al "Near-infrared multi-wavelengths long persistent luminescence of Nd3+ ion through persistent energy transfer in Ce3+, Cr3+ co-doped Y3Al2Ga3O12 for the first and second bio-imaging windows" Applied Phys. Letters 10, 8, 081903 (2015).

[11] Bos, A.J.J.; Dorenbos, P., Bessiere, A., Viana, B. et al. "Lanthanide energy levels in YPO4" Radiation Measurements, 43, 2-6, 222-226 (2008).

[12] Zhuang, Y., Katayama, Y., Ueda, J., Tanabe, S. "A brief review on red to near-infrared persistent luminescence in transition-metal-activated phosphors", Optical Materials, 36, 1907–1912 (2014).

[13] Xu, J.; Ueda, J.; Zhuang, Y.; et al. "Y3Al5-xGaxO12:Cr3+: A novel red persistent phosphor with high brightness" Applied Phys. Express 8, 4 042602 (2015).

[14] Frangioni, J.V. "In vivo near-infrared fluorescence imaging"; Curr. Opin. Chem. Biol., 7, 626–634 (2003).

[15] Cheong, W.F., Prahl, S.A., Welch, A.J. "A review of the optical properties of biological tissues"; IEEE J. Quantum Electron., 26, 2166–2185 (1990).

[16] Le Masne de Chermont, Q., Chanéac, C., Seguin, J., Pellé, F., Maitrejean, S., Jolivet, J. P., Gourier, D., Bessodes, M., Scherman, D. "Nanoprobes with near-infrared persistent luminescence for in vivo imaging"; Proc. Natl. Acad. Sci. USA, 104, 9266–9271 (2007).

[17] Rosticher, C., Viana, B., Laurent, G., Le Griel, P., Chanéac, C. "Insight into $CaMgSi_2O_6$:Eu^{2+},Mn^{2+},Dy^{3+} nanoprobes: influence of chemical composition and crystallinity on persistent red luminescence"; Eur. J. Inorg. Chem., 3681–3687 (2015).

[18] Stöber, W., Fink, A., Bohn, E. "Controlled Growth of Monodisperse Silica spheres in the Micron Size Range"; Journal of colloid and interface science, 26, 62 (1968).

[19] Lecointre, A., Bessière, A., Viana, B., Gourier, D. "Red persistent luminescent silicate nanoparticles"; Radiation Measurements, 45, 497–499 (2010).

[20] Lecointre, A., Bessière, A., Priolkar, K.R., Gourier, D., Wallez, G., Viana, B. "Role of manganese in red long-lasting phosphorescence of manganese-doped diopside for in vivo imaging"; Materials Research Bulletin, 48, 1898–1905 (2013).

[21] Bessiere, A., Lecointre, A., Priolkar, K.R., Gourier, D. "Role of crystal defects in red long-lasting phosphorescence of $CaMgSiO_2$:Mn diopsides"; J. of Mater. Chem., 22, 19039–19046 (2012).

[22] Poldervaart, A.J., Hess, H.H. "Pyroxenes in the crystallization of basaltic magma"; J. Geology., 59, 472–489 (1951).

[23] Brown, W.L., Morimoto, N., Smith, J.V. "A structural explanation of the polymorphism and transitions of $MgSiO_3$"; J. Geology., 69, 609–616 (1961).

[24] Bessiere, A., Lecointre, A., Benhamou, R.; et al., "How to induce red persistent luminescence in biocompatible Ca-3(PO4)(2) " J. of Mat. Chem. C, 1, 6, 1252-1259 (2013).